

Analysis of Elastic-Plastic Waves in a Thin-Walled Tube By a Novel Lie-Group Differential Algebraic Equations Method

Chein-Shan Liu¹ and Satya N. Atluri²

Abstract: In this paper, we adopt the viewpoint of a nonlinear complementarity problem (NCP) to derive an index-one differential algebraic equations (DAEs) system for the problem of elastic-plastic wave propagation in an elastic-plastic solid undergoing small deformations. This is achieved by recasting the pointwise complementary trio in the elastic-plastic constitutive equations into an algebraic equation through the Fischer-Burmeister NCP-function. Then, for an isotropically-hardening/softening material under prescribed impulse loadings on a thin-walled tube with combined axial-torsional stresses, we can develop a novel algorithm based on the Lie-group differential algebraic equations (LGDAE) method to iteratively solve the resultant DAEs at each time marching step, which converges very fast. The one-dimensional axial-torsional wave propagation problems under different imposed dynamical loading conditions and initial conditions are solved, to assess the performance of the LGDAE.

Keywords: Elastoplasticity, Lie-group $GL(n, \mathbb{R})$, Index-one differential algebraic equations, Elastic-plastic wave, Lie-group differential algebraic equations (LGDAE) method.

1 Introduction

The combined axial and torsional testing of thin-walled tubes is ideal for the study of constitutive equations of metals; see, for example, Nadai (1950) and Hill (1950). The thin-walled tubular specimen is usually subjected to a combination of axial load $P(t)$ and torque $T(t)$. With an appropriate feedback arrangement, the length $Z(t)$ and the relative twist angle $\Theta(t)$, as well as $P(t)$ and $T(t)$ can serve as control variables. Thus the axial-torsional testing of a thin-walled tube may have (P, T) ,

¹ Department of Civil Engineering, National Taiwan University, Taipei, Taiwan.
E-mail: liucs@ntu.edu.tw

² Center for Aerospace Research & Education, University of California, Irvine, USA.

(Z, Θ) , (P, Θ) , and (Z, T) as control input pairs. Under the assumption of uniform deformation and stress distribution in the main parallel segment of the thin wall of the specimen, the four control pairs can be correspondingly related to $(\sigma_{xx}, \sigma_{x\theta})$, $(\epsilon_{xx}, \epsilon_{x\theta})$, $(\sigma_{xx}, \epsilon_{x\theta})$, and $(\epsilon_{xx}, \sigma_{x\theta})$. They are, respectively, pure stress control, s-strain control, and mixed controls; see, for example, Klisinski, Mroz and Runesson (1992). In a small deformation theory, the stress and strain paths for the considered tests are such that their rates are of the forms:

$$\dot{\sigma} = \begin{bmatrix} \dot{\sigma}_{11} & \dot{\sigma}_{12} & 0 \\ \dot{\sigma}_{12} & 0 & 0 \\ 0 & 0 & 0 \end{bmatrix}, \quad \dot{\epsilon} = \begin{bmatrix} \dot{\epsilon}_{11} & \dot{\epsilon}_{12} & 0 \\ \dot{\epsilon}_{12} & \dot{\epsilon}_{22} & 0 \\ 0 & 0 & \dot{\epsilon}_{22} \end{bmatrix}, \quad (1)$$

where the superimposed dot denotes a differentiation with respect to time t . Notice that $\dot{\sigma}_{21} = \dot{\sigma}_{12}$, $\dot{\epsilon}_{21} = \dot{\epsilon}_{12}$, and $\dot{\epsilon}_{33} = \dot{\epsilon}_{22}$. In cylindrical coordinates (x, θ, r) , $\epsilon_{11} = \epsilon_{xx}$ is the axial strain, $\epsilon_{22} = \epsilon_{\theta\theta}$ is the hoop (or circumferential) strain, $\epsilon_{33} = \epsilon_{rr}$ is the radial strain, and $\epsilon_{12} = \epsilon_{x\theta}$ is the shear strain in the thin wall of the tube, whereas $\sigma_{11} = \sigma_{xx}$ is the axial stress and $\sigma_{12} = \sigma_{x\theta}$ is the shear stress in the thin wall of the tube.

The experiments involving combined longitudinal and torsional plastic waves in a thin-walled tube of an aluminum alloy have been reported by Lipkin and Clifton (1970a). Two types of plastic waves were observed, which involved coupled longitudinal and torsional motions. In the course of an impulse loading, the metallic material behaves plastically when stress is over the yield point, and the phenomenon of stress wave propagation in elastic-plastic solids has been studied for a long time [Cristescu (1967); Nowacki (1978)]. In an earlier analytical work, Clifton (1966) has considered the combined longitudinal and torsional plastic wave propagation in isotropically-hardening materials, and these two waves are called fast and slow plastic waves depending on whether the plastic wave speed is greater or less than the elastic shear wave speed. The analysis was extended by Lipkin and Clifton (1970b) to the general class of elastic-plastic materials characterized by a smooth loading surface. Goel and Malvern (1970) presented solutions to the same problem for the case of combined kinematic and isotropic hardening materials. Most theoretical results and computational techniques are based on the method of characteristics [Yang (1970); Ting (1969, 1972, 1973); Wu and Lin (1974); Lin and Ballmann (1993); Karagiozova (2004)]; however, it is not easy to determine the speeds of characteristic lines which are dependent on the loading history for elastic-plastic material. Unfortunately, these analyses cannot be applied to the stress wave propagation when wave reflection occurs at the boundary [Tanimoto (2007)].

It is known that the elastoplastic equations are a set of differential algebraic equations (DAEs) with discontinuities, which take place at the points of transition from

an elastic state to a plastic state and vice versa [Büttner and Simeon (2002); Eckert, Baaser, Gross and Scherf (2004)]. Most practical problems of wave propagation in such a complicated situation cannot be solved analytically due to the shape of the boundaries, the hardening effect and the complicated loading functions. Owing to these facts, the elastic-plastic wave equation is not a pure conservation law. Although there exist many numerical schemes for hyperbolic conservation laws, which cannot be directly used to solve the elastic-plastic wave equations and some modifications are required [Giese and Fey (2003, 2005)].

In the present theoretical computation of the elastic-plastic wave propagations in a solid material, we place a greater emphasis on a unified point-of-view under the framework of a Lie-group differential algebraic equations (LGDAE) method, which is drastically different from the above mentioned methods. It is important to note that unlike most other numerical schemes, the present method can be easily extended to the approximations of any order in space and time and any complicated elasto-plastic model with complex hardening/softening effect [Liu (2005, 2006, 2007); Liu and Chang (2004)], which is extremely advantageous for a high-accuracy solution of the elastic-plastic wave propagation problems.

The remainder of this paper is structured as follows. In Section 2 we emphasize the complementary trio appearing in a system of six postulations for isotropically-hardening plasticity, in tensor form. Then, in Section 3 we introduce the Fischer-Burmeister NCP-function, and propose a novel system of index-one DAEs for the isotropically-hardening plasticity equations, where we describe the governing equations, nonlinear complementarity problem, and momentum balance equation for a thin-walled tube problem. These equations are coined as a system of DAEs for all material points. For solving the resultant DAEs we develop a Lie-group method based on $GL(n, \mathbb{R})$ in Section 4, while the numerical algorithm for the elastic-plastic wave propagation problem of the isotropically-hardening plasticity is given in Section 5. In Section 6 we study the wave propagation problems of an exponentially saturated hardening material, an isotropically linear hardening material, as well as an isotropically softening material under different loading conditions, by using the corresponding LGDAE numerical algorithm. Finally, some conclusions are drawn in Section 7.

2 The isotropically-hardening model

In a small-deformation theory, the elastoplastic model for solid materials proposed by Prandtl (1924) and Reuss (1930) is re-formulated as follows:

$$\dot{\boldsymbol{\varepsilon}} = \dot{\boldsymbol{\varepsilon}}^e + \dot{\boldsymbol{\varepsilon}}^p, \quad (2)$$

$$\dot{\sigma} = 2G\dot{\varepsilon}^e + \frac{3K-2G}{3}(\text{tr}\dot{\varepsilon})\mathbf{I}, \quad (3)$$

$$\dot{\varepsilon}^p = \frac{\lambda \left[\sigma - \frac{1}{3}(\text{tr}\sigma)\mathbf{I} \right]}{2\tau_y}, \quad (4)$$

$$\sqrt{\frac{1}{2} \left[\sigma - \frac{1}{3}(\text{tr}\sigma)\mathbf{I} \right] \cdot \left[\sigma - \frac{1}{3}(\text{tr}\sigma)\mathbf{I} \right]} \leq \tau_y, \quad (5)$$

$$\lambda \geq 0, \quad (6)$$

$$\lambda \sqrt{\frac{1}{2} \left[\sigma - \frac{1}{3}(\text{tr}\sigma)\mathbf{I} \right] \cdot \left[\sigma - \frac{1}{3}(\text{tr}\sigma)\mathbf{I} \right]} = \lambda \tau_y, \quad (7)$$

where \mathbf{I} is the third-order identity tensor, the symbol tr denotes the trace of the tensor, and a dot between two tensors of the same order denotes their Euclidean inner product. The model has only two experimentally determined material constants and a material property, namely the bulk modulus K , the shear modulus G , and the shear yield strength τ_y , which are postulated to be

$$\frac{1}{K} \geq 0, \quad G > 0, \quad \tau_y > 0. \quad (8)$$

τ_y is supposed to be a function of Λ where $\dot{\Lambda} = \lambda$, $\Lambda(0) = 0$. The boldfaced ε , ε^e , ε^p and σ are, respectively, the strain, elastic strain, plastic strain, and stress tensors, all symmetric, whereas λ is a scalar. All the ε , ε^e , ε^p , σ and λ are functions of one and the same independent variable, which in most cases is taken as the ordinary time.

3 Axial-torsional plastic wave

3.1 Governing equations

For a two-dimensional axial-torsional deformation problem the following constitutive equations can be obtained from Eqs. (2)-(4) and (1),

$$\dot{\sigma}_{11} = E\dot{\varepsilon}_{11} - \frac{E\lambda}{3\tau_y}\sigma_{11}, \quad (9)$$

$$\dot{\sigma}_{12} = 2G\dot{\varepsilon}_{12} - \frac{G\lambda}{\tau_y}\sigma_{12}, \quad (10)$$

and the yield condition reduces to

$$\left(\frac{\sigma_{11}}{\sqrt{3}}\right)^2 + \sigma_{12}^2 = \tau_y^2. \tag{11}$$

We may use Eqs. (9) and (10) to solve for σ_{11} and σ_{12} , respectively. However, they are coupled through Eq. (11), where τ_y is not a constant value, but a function of Λ with $\dot{\Lambda} = \lambda$.

3.2 Nonlinear complementarity problem

A general complementarity problem is to find a solution $\mathbf{x} \in \mathbb{R}^n$ of the following complementary trio system:

$$\mathbf{P}(\mathbf{x}) \geq \mathbf{0}, \quad \mathbf{Q}(\mathbf{x}) \geq \mathbf{0}, \quad \mathbf{P}^T \mathbf{Q} = \mathbf{0}, \tag{12}$$

where $\mathbf{P}, \mathbf{Q} \in \mathbb{R}^n$ denote vector functions. Many applications from engineering sciences, economics, game theory, etc. lead to problems of this kind; see Ferris and Pang (1997) for a survey. Most algorithms for the solution of nonlinear complementarity problem (NCP) are based on a suitable reformulation of Eq. (12) either as a system of algebraic equations, as an optimization problem, or as a fixed-point problem, etc. Refer the survey paper by Harker and Pang (1990) for some basic algorithms.

Let x be a solution of an NCP, that is, $x \geq 0$, $F(x) \geq 0$, and $x F(x) = 0$. Obviously, it is equivalent to the requirement that x is a solution of the minimum problem: $\min(x, F(x)) = 0$. The function ϕ is said to be an NCP-function: if $\phi : \mathbb{R}^2 \mapsto \mathbb{R}$ and $\phi(a, b) = 0$ if and only if $a \geq 0$, $b \geq 0$, $ab = 0$.

In addition to the above minimum function, there are many other NCP-functions, for example, the Fischer-Burmeister NCP-function:

$$\phi_{\text{FB}}(a, b) = \sqrt{a^2 + b^2} - (a + b). \tag{13}$$

The most interesting property of this merit function is that, as is easily verified:

$$\sqrt{a^2 + b^2} - (a + b) = 0 \iff a \geq 0, \quad b \geq 0, \quad ab = 0. \tag{14}$$

Thus, for a general NCP of Eq. (12) in a component form we write it to be

$$F_i = \phi_{\text{FB}}(P_i, Q_i) = \sqrt{P_i^2 + Q_i^2} - (P_i + Q_i) = 0, \quad i = 1, \dots, n, \tag{15}$$

where P_i and Q_i are respectively the components of \mathbf{P} and \mathbf{Q} . Accordingly, we can reformulate the complementary trio in plasticity as an NCP by

$$\dot{\sigma}_{11} = E\dot{\varepsilon}_{11} - \frac{E\lambda}{3\tau_y(\Lambda)}\sigma_{11}, \quad (16)$$

$$\dot{\sigma}_{12} = 2G\dot{\varepsilon}_{12} - \frac{G\lambda}{\tau_y(\Lambda)}\sigma_{12}, \quad (17)$$

$$\dot{\Lambda} = \lambda, \quad (18)$$

$$\sqrt{\left[\tau_y(\Lambda) - \sqrt{\left(\frac{\sigma_{11}}{\sqrt{3}}\right)^2 + \sigma_{12}^2} \right]^2 + \lambda^2} - \left[\tau_y(\Lambda) - \sqrt{\left(\frac{\sigma_{11}}{\sqrt{3}}\right)^2 + \sigma_{12}^2} \right] - \lambda = 0. \quad (19)$$

It is easy to check that Eqs. (16)-(19) are index-one DAEs, which are better than those of the index-two DAEs formulation of plasticity [Büttner and Simeon (2003a, 2003b); Liu (2013c)]. On the other hand, in Eqs. (16)-(19) we do not need to treat the on-off switch, while for the original index-two DAEs we need to treat a two-phase system and the on-off switching criteria of elasticity and plasticity.

3.3 Kinematic and momentum balance equation

Our method is easily extended to the three-dimensional elastic-plastic wave propagation problem by adjoining the momentum balance equation together:

$$\nabla \cdot \boldsymbol{\sigma} = \rho \frac{\partial \mathbf{w}}{\partial t}, \quad (20)$$

where ρ is the material density while \mathbf{w} is the velocity field. However, we only consider the process of the propagation of an elastic-plastic wave in a finite length thin-walled tube with length ℓ consisting of an isotropically hardening material, subjected to dynamical boundary conditions and initial conditions. The problem will be discussed in a Lagrangian system where the axis x coincides with the thin-walled tube axis, and the origin $x = 0$ is assumed to be the left-end point of the thin-walled tube. It is also assumed that the thin-walled tube does not buckle in the course of deformation. We consider small strains and assume that the thin-walled tube density ρ does not change. The only stress components are $\sigma_{xx} = \sigma$ and $\sigma_{x\theta} = \tau$, and the non-zero strain components are $\varepsilon_{xx} = \varepsilon$, $\varepsilon_{x\theta} = \gamma/2$, and $\varepsilon_{rr} = \varepsilon_{\theta\theta}$. The velocity field has only the first two components being nonzero and the third

component is zero, i.e., $\mathbf{w} = (u, v, 0)^T$. Hence, the governing equations at a material point x and a generic time t can be written as

$$\frac{\partial \sigma(x, t)}{\partial t} = E \frac{\partial u(x, t)}{\partial x} - \frac{\lambda(x, t)E}{3\tau_y(\Lambda)} \sigma(x, t), \quad (21)$$

$$\frac{\partial \tau(x, t)}{\partial t} = G \frac{\partial v(x, t)}{\partial x} - \frac{\lambda(x, t)G}{\tau_y(\Lambda)} \tau(x, t), \quad (22)$$

$$\frac{\partial u(x, t)}{\partial t} = \frac{1}{\rho} \frac{\partial \sigma(x, t)}{\partial x}, \quad (23)$$

$$\frac{\partial v(x, t)}{\partial t} = \frac{1}{\rho} \frac{\partial \tau(x, t)}{\partial x}, \quad (24)$$

$$\frac{\partial \Lambda(x, t)}{\partial t} = \lambda(x, t), \quad (25)$$

$$\sqrt{\left[\tau_y(\Lambda) - \sqrt{\left(\frac{\sigma}{\sqrt{3}} \right)^2 + \tau^2} \right]^2 + \lambda^2} - \left[\tau_y(\Lambda) - \sqrt{\left(\frac{\sigma}{\sqrt{3}} \right)^2 + \tau^2} \right] - \lambda = 0, \quad (26)$$

where u and v are the axial and circumferential velocities.

If we want to know the field variables of strains $\varepsilon(x, t)$ and $\gamma(x, t)$ we can supplement the following kinematic equations:

$$\frac{\partial \varepsilon(x, t)}{\partial t} = \frac{\partial u(x, t)}{\partial x}, \quad (27)$$

$$\frac{\partial \gamma(x, t)}{\partial t} = \frac{\partial v(x, t)}{\partial x}. \quad (28)$$

4 A Lie-group DAE method

After a suitable discretization of the above equations at each material point, Eqs. (21)-(26) constitute a system of nonlinear differential algebraic equations (DAEs). Hereby, we give a general setting to treat the DAEs which govern the evolution of $n + q$ variables x_i , $i = 1, \dots, n$ and y_j , $j = 1, \dots, q$, with n nonlinear ordinary differential equations (ODEs) and q nonlinear algebraic equations (NAEs):

$$\dot{\mathbf{x}} = \mathbf{f}(\mathbf{x}, \mathbf{y}, t), \quad \mathbf{x}(0) = \mathbf{x}_0, \quad t \in \mathbb{R}, \quad \mathbf{x} \in \mathbb{R}^n, \quad \mathbf{y} \in \mathbb{R}^q, \quad (29)$$

$$\mathbf{F}(\mathbf{x}, \mathbf{y}, t) = \mathbf{0}, \quad \mathbf{F} \in \mathbb{R}^q. \quad (30)$$

4.1 Endowing the ODEs with a Lie-group $GL(n, \mathbb{R})$

The general linear group is a Lie group, whose manifold is an open subset $GL(n, \mathbb{R}) : = \{\mathbf{G} \in \mathbb{R}^{n \times n} | \det \mathbf{G} \neq 0\}$ of the linear space of all $n \times n$ non-singular matrices. Thus, $GL(n, \mathbb{R})$ is an $n \times n$ -dimensional manifold. The group composition is given by the matrix multiplication.

Here we give a new form of Eq. (29) from the $GL(n, \mathbb{R})$ Lie-group structure. The vector field \mathbf{f} on the right-hand side of Eq. (29) can be written as

$$\dot{\mathbf{x}} = \mathbf{A}\mathbf{x}, \quad (31)$$

where

$$\mathbf{A} = \frac{\mathbf{f}}{\|\mathbf{x}\|} \otimes \frac{\mathbf{x}}{\|\mathbf{x}\|} \quad (32)$$

is the coefficient matrix. The symbol \otimes in $\mathbf{u} \otimes \mathbf{y}$ denotes the dyadic operation of \mathbf{u} and \mathbf{y} , i.e., $(\mathbf{u} \otimes \mathbf{y})\mathbf{z} = \mathbf{y} \cdot \mathbf{z}\mathbf{u}$.

Because the coefficient matrix \mathbf{A} is well-defined, the Lie-group element \mathbf{G} generated from the above dynamical system (31) with $\dot{\mathbf{G}} = \mathbf{A}\mathbf{G}$ satisfies $\det \mathbf{G}(t) \neq 0$, such that $\mathbf{G} \in GL(n, \mathbb{R})$.

Liu (2013a) has found the essential form in Eq. (31) for nonlinear ODEs, and developed a very effective Lie-group $GL(n, \mathbb{R})$ scheme to solve ODEs by only assuming that $\mathbf{f}/\|\mathbf{x}\|$ is a constant vector within a small time step. Then, Liu (2013b) developed a Lie-group $GL(n, \mathbb{R})$ scheme to solve ODEs by assuming that both $\mathbf{f}/\|\mathbf{x}\|$ and $\mathbf{x}/\|\mathbf{x}\|$ are constant vectors in a small time incremental step. Liu (2013c) has developed a powerful numerical method to solve the nonlinear differential algebraic equations, based on the above Lie-group $GL(n, \mathbb{R})$ scheme. Liu (2014a) has used the Lie-group differential algebraic equations (LGDAE) method to solve the sliding mode control problem, and Liu (2014b) has solved the heat source identification problem by using the LGDAE.

4.2 An implicit $GL(n, \mathbb{R})$ Lie-group scheme

Eq. (31) is a new starting point for the development of the Lie-group $GL(n, \mathbb{R})$ algorithm. In order to develop a numerical scheme from Eqs. (31) and (32), we suppose that the coefficient matrix \mathbf{A} is constant with

$$\mathbf{a} = \frac{\bar{\mathbf{f}}}{\|\bar{\mathbf{x}}\|}, \quad \mathbf{b} = \frac{\bar{\mathbf{x}}}{\|\bar{\mathbf{x}}\|} \quad (33)$$

being two constant vectors, which can be obtained by taking the values of \mathbf{f} and \mathbf{x} at a suitable mid-point of $\bar{t} \in [t_0 = 0, t]$, where $t \leq t_0 + h$ and h is a small time stepsize.

The variable \mathbf{y} is suppose to be a constant vector in this small time interval. Thus from Eqs. (31) and (32) we have

$$\dot{\mathbf{x}} = \mathbf{b} \cdot \mathbf{x}\mathbf{a}. \tag{34}$$

By defining

$$w = \mathbf{b} \cdot \mathbf{x}, \tag{35}$$

Eq. (34) becomes

$$\dot{\mathbf{x}} = w\mathbf{a}. \tag{36}$$

Then, from the above two equations we can derive

$$\dot{w} = cw, \tag{37}$$

where

$$c = \mathbf{a} \cdot \mathbf{b} \tag{38}$$

is a constant scalar in a small time step. From Eq. (37) it follows that

$$w(t) = w_0 \exp(ct), \tag{39}$$

where $w_0 = \mathbf{b} \cdot \mathbf{x}_0$.

Inserting Eq. (39) for $w(t)$ into Eq. (36) and integrating the resultant equation we can obtain

$$\mathbf{x}(t) = [\mathbf{I}_n + \eta(t)\mathbf{a}\mathbf{b}^T]\mathbf{x}_0, \tag{40}$$

where the superscript τ denotes the transpose, \mathbf{x}_0 is the initial value of \mathbf{x} at an initial time $t = t_0 = 0$, and

$$\eta(t) = \frac{e^{ct} - 1}{c}. \tag{41}$$

Let \mathbf{G} be the coefficient matrix before \mathbf{x}_0 in Eq. (40):

$$\mathbf{G} = \mathbf{I}_n + \eta\mathbf{a}\mathbf{b}^T, \tag{42}$$

which is one sort of elementary matrices. According to Liu (2013a, 2013c) we can prove

$$\det \mathbf{G} = e^{ct} > 0, \tag{43}$$

such that \mathbf{G} is a Lie-group element of $GL(n, \mathbb{R})$.

Within a small time step we can suppose that the variables y_j , $j = 1, \dots, m$ are constant in the interval of $t_k < t < t_{k+1}$. Consequently, we can develop the following implicit scheme for solving the ODEs (29) where \mathbf{y} at the k th time step, denoted by \mathbf{y}_k , is viewed as parameters:

- (i) Give $0 \leq \theta \leq 1$.
- (ii) Give an initial \mathbf{x}_0 at an initial time $t = t_0$ and a time stepsize h .
- (iii) For $k = 0, 1, \dots$, we repeat the following computations to a terminal time:

$$\mathbf{x}_{k+1} = \mathbf{x}_k + h\mathbf{f}_k, \quad (44)$$

where $\mathbf{f}_k := \mathbf{f}(\mathbf{x}_k, \mathbf{y}_k, t_k)$. With the above \mathbf{x}_{k+1} generated from an Euler step as an initial guess we can iteratively solve the new \mathbf{x}_{k+1} by

$$\begin{aligned} \bar{t}_k &= t_k + \theta h, \\ \bar{\mathbf{x}}_k &= (1 - \theta)\mathbf{x}_k + \theta\mathbf{x}_{k+1}, \\ \bar{\mathbf{f}}_k &= \mathbf{f}(\bar{\mathbf{x}}_k, \mathbf{y}_k, \bar{t}_k), \\ \mathbf{a}_k &= \frac{\bar{\mathbf{f}}_k}{\|\bar{\mathbf{x}}_k\|}, \\ \mathbf{b}_k &= \frac{\bar{\mathbf{x}}_k}{\|\bar{\mathbf{x}}_k\|}, \end{aligned} \quad (45)$$

$$\begin{aligned} c_k &= \mathbf{a}_k \cdot \mathbf{b}_k, \\ d_k &= \mathbf{x}_k \cdot \mathbf{b}_k, \\ \eta_k &= \frac{\exp(c_k h) - 1}{c_k}, \\ \mathbf{z}_{k+1} &= \mathbf{x}_k + \eta_k d_k \mathbf{a}_k. \end{aligned} \quad (46)$$

If \mathbf{z}_{k+1} converges according to a given stopping criterion, such that,

$$\|\mathbf{z}_{k+1} - \mathbf{x}_{k+1}\| < \varepsilon_2, \quad (47)$$

then go to (iii) to the next time step; otherwise, let $\mathbf{x}_{k+1} = \mathbf{z}_{k+1}$ and go to the computations in Eqs. (45)-(46) again. In all the computations given below we will fix $\theta = 1/2$.

4.3 Newton iterative scheme for DAEs

Now, we turn our attention to the DAEs defined in Eqs. (29) and (30). Within a small time step we can suppose that the variables y_j , $j = 1, \dots, m$ are constant in

the interval of $t_k < t < t_{k+1}$. We give an initial guess of y_j , $j = 1, \dots, m$, and insert them into Eq. (29). Then we apply the above implicit scheme to find the next \mathbf{x}_{k+1} , supposing that \mathbf{x}_k is already obtained in the previous time step. When \mathbf{x}_{k+1} are available we insert them into Eq. (30), and then apply the Newton iterative scheme to solve \mathbf{y}_{k+1} by

$$\mathbf{y}_{k+1}^{\ell+1} = \mathbf{y}_{k+1}^{\ell} - \mathbf{B}^{-1} \mathbf{F}(\mathbf{x}_{k+1}, \mathbf{y}_{k+1}^{\ell}, t_{k+1}), \quad (48)$$

till the following convergence criterion is satisfied:

$$\|\mathbf{y}_{k+1}^{\ell+1} - \mathbf{y}_{k+1}^{\ell}\| < \varepsilon_1. \quad (49)$$

Otherwise, go to Eq. (45). In the above the component B_{ij} of the Jacobian matrix \mathbf{B} is given by $\partial F_i / \partial y_j$.

The numerical process as a combination of the Lie-group method based on $GL(n, \mathbb{R})$ and the Newton method to solve the DAEs in Eqs. (29) and (30) is called the Lie-group DAE (LGDAE) method.

5 Numerical algorithm for elastic-plastic wave

Now we suppose that all the variables are discretized to be $\sigma_i(t) = \sigma(x_i, t)$, $\tau_i(t) = \tau(x_i, t)$, $u_i(t) = u(x_i, t)$, $v_i(t) = v(x_i, t)$, $\lambda_i(t) = \lambda(x_i, t)$ and $\Lambda_i(t) = \Lambda(x_i, t)$, where $x_i = (i-1)\Delta x = (i-1)\ell / (m-1)$, and m is the number of grid points. Then, we have totally $n = 5m$ ODEs and $q = m$ constraints:

$$\dot{\sigma}_1(t) = -E \frac{3u_1(t) - 4u_2(t) + u_3(t)}{2\Delta x} - \frac{\lambda_1(t)E}{3\tau_y(\Lambda_1)} \sigma_1(t), \quad i = 1,$$

$$\dot{\sigma}_i(t) = E \frac{u_{i+1}(t) - u_{i-1}(t)}{2\Delta x} - \frac{\lambda_i(t)E}{3\tau_y(\Lambda_i)} \sigma_i(t), \quad i = 2, \dots, m-1,$$

$$\dot{\sigma}_m(t) = E \frac{3u_m(t) - 4u_{m-1}(t) + u_{m-2}(t)}{2\Delta x} - \frac{\lambda_m(t)E}{3\tau_y(\Lambda_m)} \sigma_m(t), \quad i = m,$$

$$\dot{\tau}_1(t) = -G \frac{3v_1(t) - 4v_2(t) + v_3(t)}{2\Delta x} - \frac{\lambda_1(t)G}{\tau_y(\Lambda_1)} \tau_1(t), \quad i = 1,$$

$$\dot{\tau}_i(t) = G \frac{v_{i+1}(t) - v_{i-1}(t)}{2\Delta x} - \frac{\lambda_i(t)G}{\tau_y(\Lambda_i)} \tau_i(t), \quad i = 2, \dots, m-1,$$

$$\dot{\tau}_m(t) = G \frac{3v_m(t) - 4v_{m-1}(t) + v_{m-2}(t)}{2\Delta x} - \frac{\lambda_m(t)G}{\tau_y(\Lambda_m)} \tau_m(t), \quad i = m,$$

$$\begin{aligned}
\dot{u}_1(t) &= -\frac{3\sigma_1(t) - 4\sigma_2(t) + \sigma_3(t)}{2\rho\Delta x}, \quad i = 1, \\
\dot{u}_i(t) &= \frac{\sigma_{i+1}(t) - \sigma_{i-1}(t)}{2\rho\Delta x}, \quad i = 2, \dots, m-1, \\
\dot{u}_m(t) &= \frac{3\sigma_m(t) - 4\sigma_{m-1}(t) + \sigma_{m-2}(t)}{2\rho\Delta x}, \quad i = m, \\
\dot{v}_1(t) &= -\frac{3\tau_1(t) - 4\tau_2(t) + \tau_3(t)}{2\rho\Delta x}, \quad i = 1, \\
\dot{v}_i(t) &= \frac{\tau_{i+1}(t) - \tau_{i-1}(t)}{2\rho\Delta x}, \quad i = 2, \dots, m-1, \\
\dot{v}_m(t) &= \frac{3\tau_m(t) - 4\tau_{m-1}(t) + \tau_{m-2}(t)}{2\rho\Delta x}, \quad i = m, \\
\dot{\Lambda}_i(t) &= \lambda_i(t), \quad i = 1, \dots, m,
\end{aligned} \tag{50}$$

$$\begin{aligned}
&\sqrt{\left[\tau_y(\Lambda_i) - \sqrt{\left(\frac{\sigma_i}{\sqrt{3}}\right)^2 + \tau_i^2} \right]^2 + \lambda_i^2} - \left[\tau_y(\Lambda_i) - \sqrt{\left(\frac{\sigma_i}{\sqrt{3}}\right)^2 + \tau_i^2} \right] - \lambda_i = 0, \\
&i = 1, \dots, m.
\end{aligned} \tag{51}$$

We apply the implicit $GL(n, \mathbb{R})$ scheme to solve σ_i , τ_i , u_i , v_i , and Λ_i through Eq. (50) and then iteratively solve the unknown function λ_i through Eq. (51) by the Newton iterative method. The numerical processes of this implicit LGDAE are given below, where we use $\mathbf{Q} = (\sigma_1, \dots, \sigma_m, \tau_1, \dots, \tau_m, u_1, \dots, u_m, v_1, \dots, v_m, \Lambda_1, \dots, \Lambda_m)^T$ and \mathbf{f} is used to denote the right-hand sides of Eq. (50):

- (i) Give an initial guess of λ_i^0 , for example, $\lambda_i^0 = 0$.
- (ii) Give an initial condition \mathbf{Q}_0 at an initial time $t = 0$ and a time stepsize δt .
- (iii) For $k = 0, 1, \dots$, we repeat the following computations to a specified terminal time $t = t_f$:

$$\mathbf{Q}_{k+1} = \mathbf{Q}_k + \delta t \mathbf{f}_k. \tag{52}$$

With the above \mathbf{Q}_{k+1} generated from an Euler step as an initial guess we then iteratively solve the new \mathbf{Q}_{k+1} by

$$\begin{aligned}
\bar{\mathbf{Q}}_k &= (1 - \theta)\mathbf{Q}_k + \theta\mathbf{Q}_{k+1}, \\
\mathbf{a}_k &= \frac{\bar{\mathbf{f}}_k}{\|\bar{\mathbf{Q}}_k\|},
\end{aligned}$$

$$\begin{aligned}
 \mathbf{b}_k &= \frac{\bar{\mathbf{Q}}_k}{\|\bar{\mathbf{Q}}_k\|}, \\
 c_k &= \mathbf{a}_k \cdot \mathbf{b}_k, \\
 d_k &= \mathbf{Q}_k \cdot \mathbf{b}_k, \\
 \eta_k &= \frac{\exp(c_k \delta t) - 1}{c_k}, \\
 \mathbf{z}_{k+1} &= \mathbf{Q}_k + \eta_k d_k \mathbf{a}_k.
 \end{aligned} \tag{53}$$

If \mathbf{z}_{k+1} converges according to a given stopping criterion, such that,

$$\|\mathbf{z}_{k+1} - \mathbf{Q}_{k+1}\| < \varepsilon_2, \tag{54}$$

then go to (iv); otherwise, let $\mathbf{Q}_{k+1} = \mathbf{z}_{k+1}$ and go to Eq. (53).

(iv) For $j = 0, 1, \dots$, we repeat the following computations:

$$\lambda_i^{j+1} = \lambda_i^j - \frac{F_i^j}{F_i^{j+1}}, \quad i = 1, \dots, m, \tag{55}$$

where the prime denotes the differential with respect to λ_i , and

$$\bar{\mathbf{f}}'_k = -\frac{E}{3\tau_y(\Lambda_k)} \bar{\mathbf{Q}}_k, \quad \text{the first } m \text{ components of } \mathbf{f} \text{ and } \mathbf{Q},$$

$$\bar{\mathbf{f}}'_k = -\frac{G}{\tau_y(\Lambda_k)} \bar{\mathbf{Q}}_k, \quad \text{the second } m \text{ components of } \mathbf{f} \text{ and } \mathbf{Q},$$

$$\bar{\mathbf{f}}'_k = 1, \quad \text{the fifth } m \text{ components of } \mathbf{f} \text{ and } \mathbf{Q},$$

$$\mathbf{a}'_k = \frac{\bar{\mathbf{f}}'_k}{\|\bar{\mathbf{Q}}_k\|},$$

$$(c_k^i)' = b_k^i (a_k^i)' + b_k^{m+i} (a_k^{m+i})' + b_k^{4m+i} (a_k^{4m+i})', \quad i = 1, \dots, m,$$

$$(\eta_k^i)' = \frac{(c_k^i)' [(c_k \delta t - 1) \exp(c_k \delta t) + 1]}{c_k^2}, \quad i = 1, \dots, m,$$

$$\begin{aligned}
(Q_{k+1}^i)' &= (\eta_k^i)' d_k a_k^i + \eta_k d_k (a_k^i)', \quad i = 1, \dots, n, \\
A_i^j &= \tau_y(\Lambda_i^j) - \sqrt{\left(\frac{\sigma_i^j}{\sqrt{3}}\right)^2 + (\tau_i^j)^2}, \quad i = 1, \dots, m, \\
F_i^j &= \sqrt{(A_i^j)^2 + (\lambda_i^j)^2} - A_i^j - \lambda_i^j, \quad i = 1, \dots, m, \\
A_i^j &= \tau_y'(\Lambda_i) - \frac{\sigma_i^j \sigma_i^{j'} / 3 + \tau_i^j \tau_i^{j'}}{\sqrt{\left(\frac{\sigma_i^j}{\sqrt{3}}\right)^2 + (\tau_i^j)^2}}, \quad i = 1, \dots, m, \\
F_i^{j'} &= \frac{A_i^j A_i^{j'} + \lambda_i^j}{\sqrt{(A_i^j)^2 + (\lambda_i^j)^2}} - A_i^{j'} - 1, \quad i = 1, \dots, m,
\end{aligned} \tag{56}$$

where both i (super or sub scripted) denote the i th components. If λ_i^j converges according to

$$|\lambda_i^{j+1} - \lambda_i^j| < \varepsilon_1, \quad i = 1, \dots, m, \tag{57}$$

then go to (iii) with λ_i^j as an initial guess of λ_i for the next time step; otherwise, let $\lambda_i^j = \lambda_i^{j+1}$ and go to Eq. (53).

6 Examples of plastic waves

In order to assess the performance of the above numerical method of LGDAE, we consider elastic-plastic wave propagation problems of a thin-walled tube with length $\ell = 0.1 \text{ m} = 100 \text{ mm}$, and the material constants are $E = 70,000 \text{ MPa}$, $G = 70,000 / [2(1 + \nu)] = 26923.08 \text{ MPa}$ with $\nu = 0.3$, and $\rho = 2700 \text{ kg/m}^3$. We consider three hardening cases and one softening case, and different loading conditions and initial conditions.

6.1 Step-loading of a linearly hardening material, comparison with Clifton (1966)

First, we consider an isotropically-linearly hardening material with τ_y being a linear function of Λ :

$$\tau_y(\Lambda) = 150 + 15000\Lambda. \tag{58}$$

The thin-walled tube is initially at rest and pre-stressed over the initial yield stress, being subjected simultaneously at the end $x = 0$ to constant stresses σ_0 and τ_0 . The

initial conditions are, respectively,

$$u(x, 0) = v(x, 0) = \tau(x, 0) = 0, \quad \sigma(x, 0) = 300, \tag{59}$$

$$u(x, 0) = v(x, 0) = \sigma(x, 0) = 0, \quad \tau(x, 0) = 250. \tag{60}$$

The thin-walled tube is pre-stressed to a plastic state and the initial value of Λ can be solved from Eq. (58). For the pre-tension case we consider $\sigma_0 = 200$ and $\tau_0 = 300$, while for the pre-shear case we consider $\sigma_0 = 350$ and $\tau_0 = 300$.

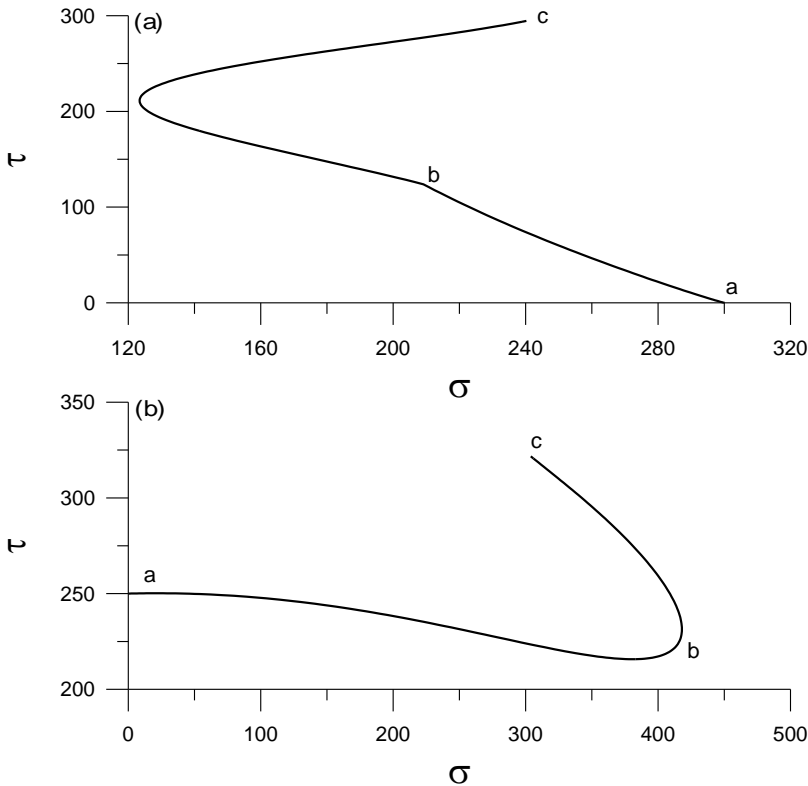


Figure 1: For an isotropically linear hardening material showing the stress paths for (a) pre-tension stress, and (b) pre-shear stress.

We fix $\Delta x = 0.01/100$ and solve this problem under a time stepsize $\delta t = 5 \times 10^{-7}$ sec in a time interval $t \in [0, 0.0001]$. The stress paths for the above two cases are plotted in Figs. 1(a) and 1(b) for a point at $x = \Delta x$. For the pre-tension case, from Fig. 1(a) it can be seen that the material quickly tends from point a to point b with a fast plastic wave where normal stress falls to a much smaller normal stress

and shear stress quickly increases from zero shear stress to a much larger shear stress, and then from point b to point c along a slow plastic wave. For the pre-shear case, from Fig. 1(b) it can be seen that the material quickly tends from point a to point b, which propagates with fast plastic wave, and then from point b to point c along a slow plastic wave. The above behaviors were described by Clifton (1966) for a semi-infinite tube by using the characteristic theory, for which our results are similar.

6.2 Exponentially saturated hardening material

We let τ_y be a function of Λ , which is given by

$$\tau_y(\Lambda) = 350 - 200\exp(-5\Lambda). \quad (61)$$

For the isotropically hardening plastic wave problem we need to calculate Λ_i by

$$\dot{\Lambda}_i(t) = \lambda_i(t), \quad i = 1, \dots, m. \quad (62)$$

Ting (1973) has analyzed the plastic wave speeds of an isotropically work hardening material.

The boundary conditions are supposed to be $u(0, t) = 1 + t + t^2$, $v(0, t) = 2(1 + t + t^2)$, and the initial conditions are given by $u(x, 0) = v(x, 0) = 0.01 \cos[(\pi x)/(2\ell)]$, and $\sigma(x, 0) = \tau(x, 0) = 50$. The right-end of the tube is fixed. We consider three different terminal times: case 1 with $t_f = 0.002$ sec, case 2 with $t_f = 0.01$ sec, and case 3 with $t_f = 0.1$ sec.

We fix $\Delta x = 0.002$ for all cases. We solve case 1 under a time stepsize $\delta t = 10^{-6}$ sec. In Fig. 2(a) we plot the elastic and plastic zones in the plane (x, t) , where the point corresponding to a plastic state is marked by a black square point. In Fig. 3 we plot the waves at some sampled times $t_1 = 500\delta t = 0.0005$ sec, $t_2 = 1000\delta t = 0.001$ sec, $t_3 = 1500\delta t = 0.0015$ sec, and $t_4 = 2000\delta t = 0.002$ sec. Then we plot the time histories of wave at two points $x_1 = 0.002$ and $x_2 = 0.08$ in Fig. 4. It can be seen that at the first point the material quickly tends to yielding and enters into the plastic state. At point x_2 the material is elastically unloading.

We solve case 2 under a time stepsize $\delta t = 5 \times 10^{-6}$ sec. In Fig. 2(b) we plot the elastic and plastic zones in the plane (x, t) . In Fig. 5 we plot the waves at some sampled times $t_1 = 10\delta t = 0.00005$ sec, $t_2 = 500\delta t = 0.0025$ sec, $t_3 = 1500\delta t = 0.0075$ sec, and $t_4 = 2000\delta t = 0.01$ sec. We plot the time histories of wave at two points $x_1 = 0.008$ and $x_2 = 0.08$ in Fig. 6. It can be seen that at the first point $x_1 = 0.008$ the material quickly tends to plastic state and intervening by elastic

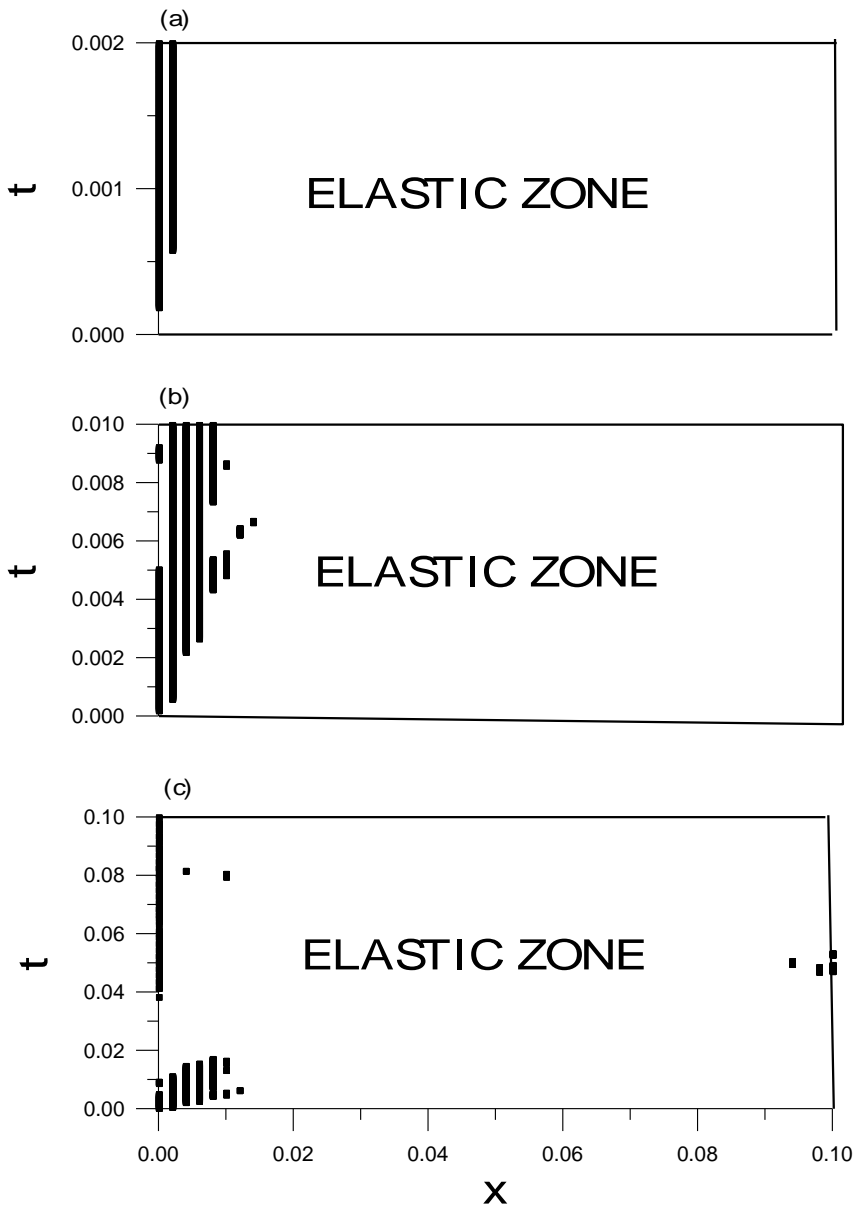


Figure 2: The elastic-plastic zones for three different terminal times for the elastic-plastic wave propagations of isotropically hardening material.

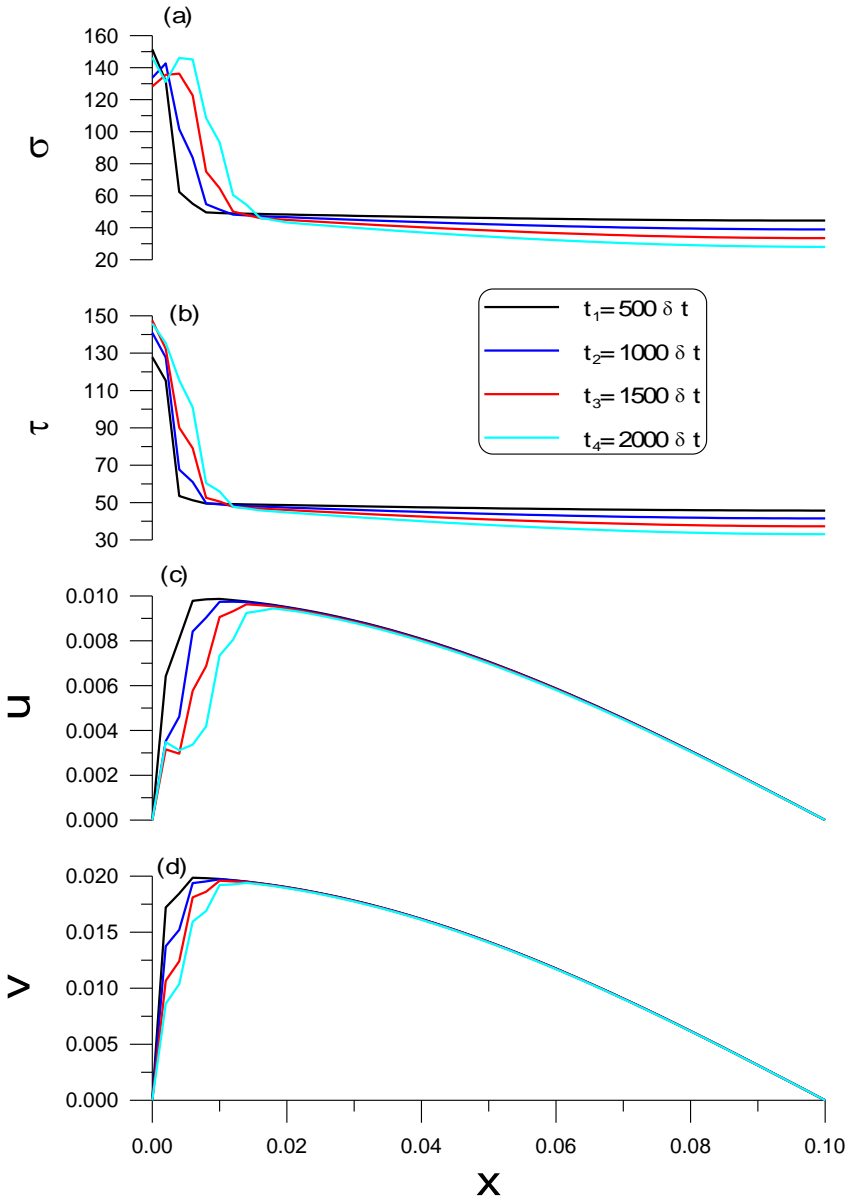


Figure 3: For case 1 the elastic-plastic wave propagation for isotropically hardening material: (a) axial stress, (b) shear stress, (c) axial velocity and (d) torsional velocity.

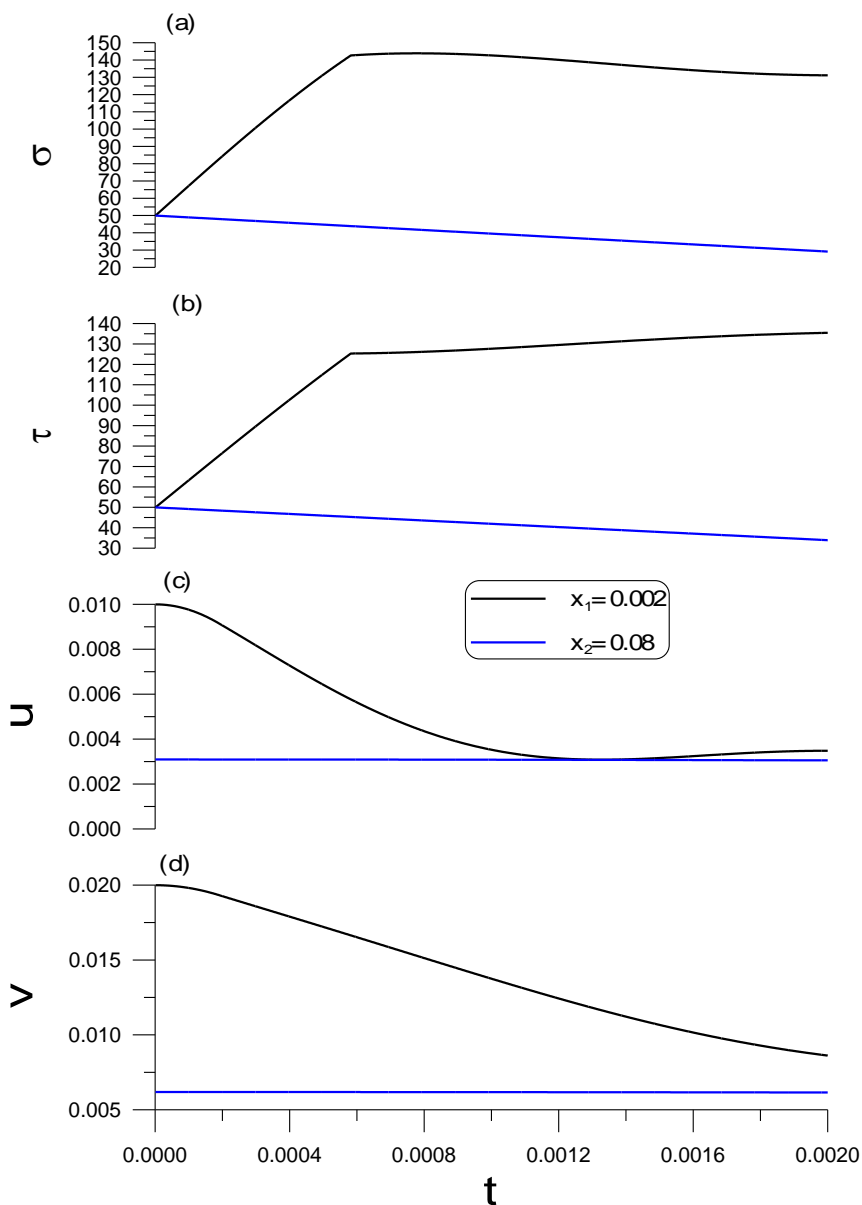


Figure 4: For case 1 of isotropically hardening material the elastic-plastic wave propagation with respect to time: (a) axial stress, (b) shear stress, (c) axial velocity, and (d) torsional velocity.

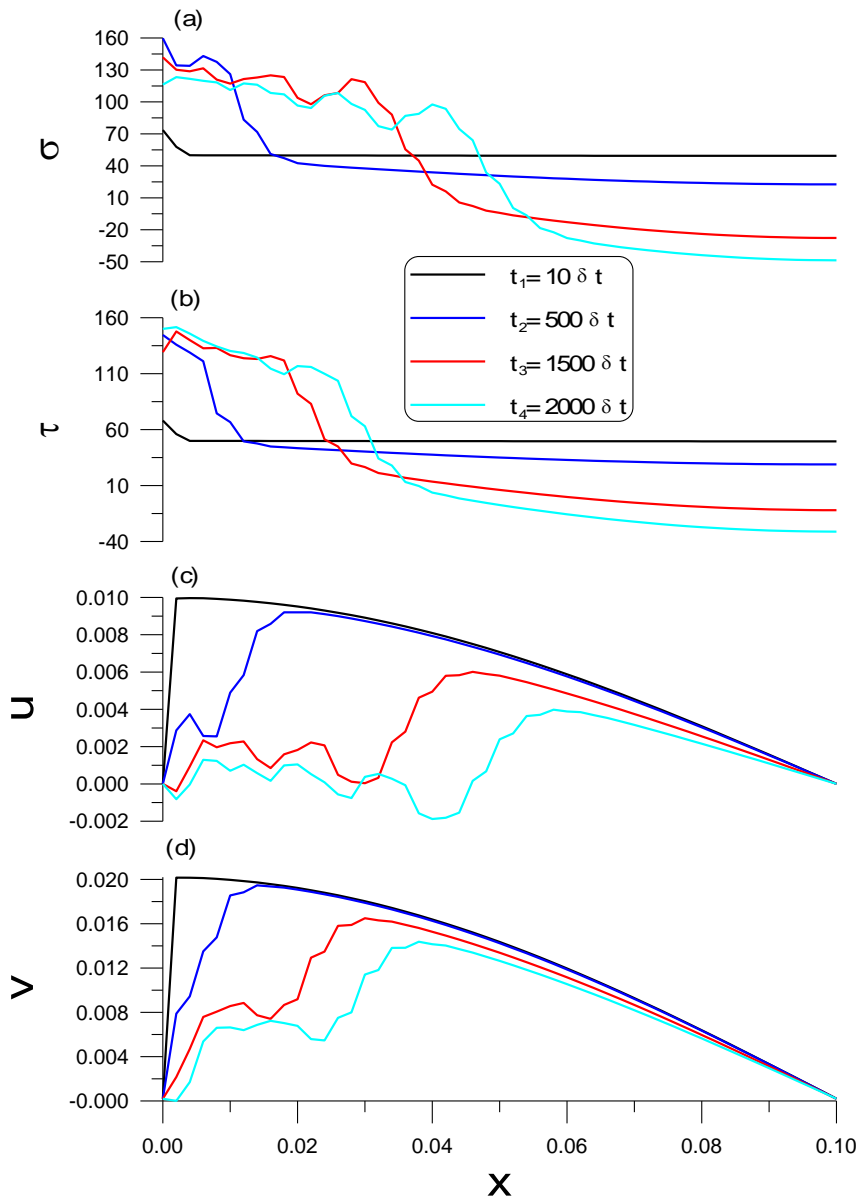


Figure 5: For case 2 the elastic-plastic wave propagation for isotropically hardening material: (a) axial stress, (b) shear stress, (c) axial velocity, and (d) torsional velocity.

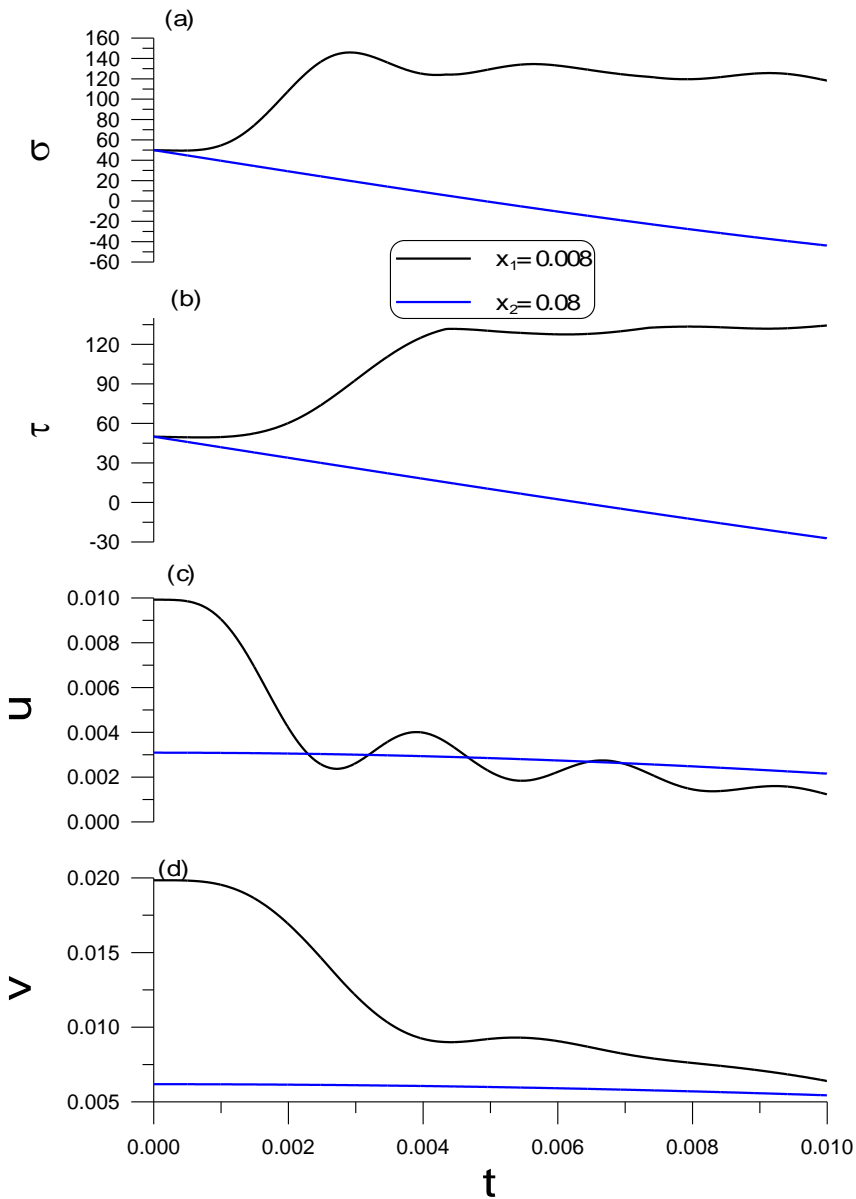


Figure 6: For case 2 of isotropically hardening material the elastic-plastic wave propagation with respect to time: (a) axial stress, (b) shear stress, (c) axial velocity, and (d) torsional velocity.

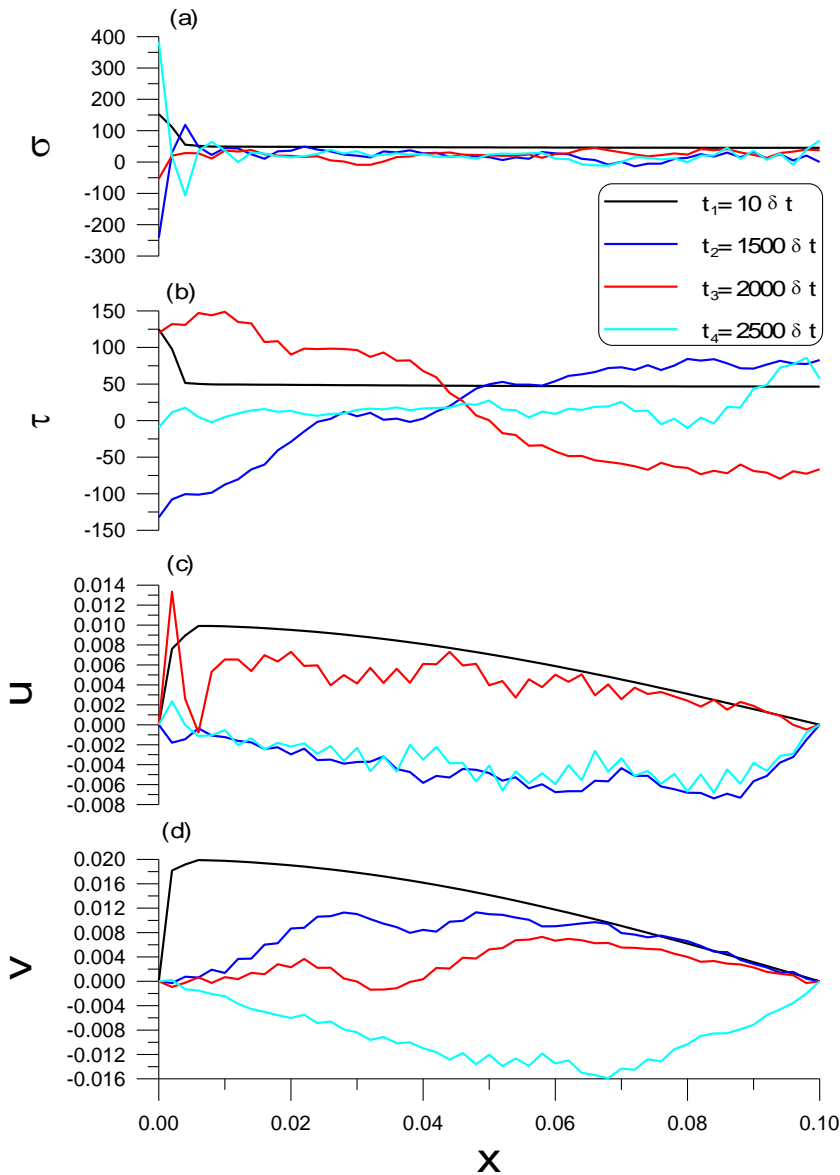


Figure 7: For case 3 the elastic-plastic wave propagation for isotropically hardening material: (a) axial stress, (b) shear stress, (c) axial velocity, and (d) torsional velocity.

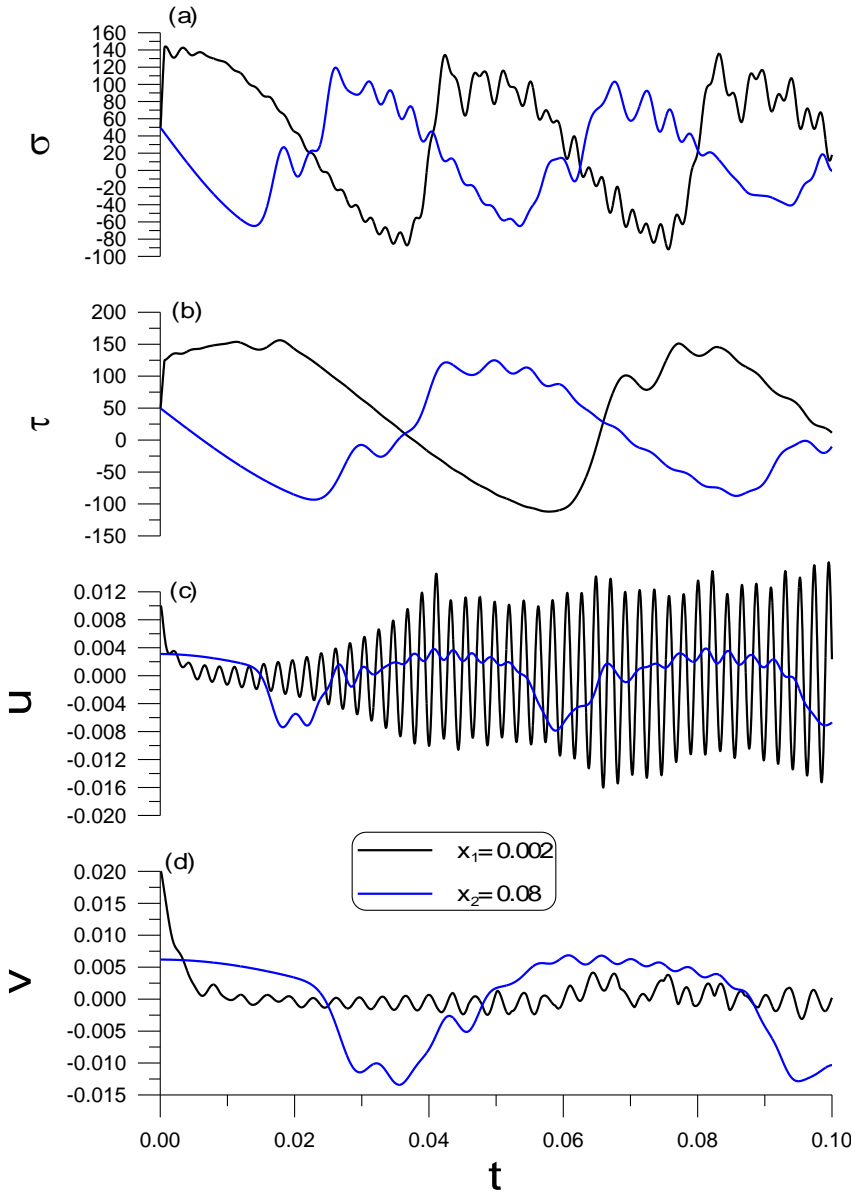


Figure 8: For case 3 of isotropically hardening material the elastic-plastic wave propagation with respect to time: (a) axial stress, (b) shear stress, (c) axial velocity, and (d) torsional velocity.

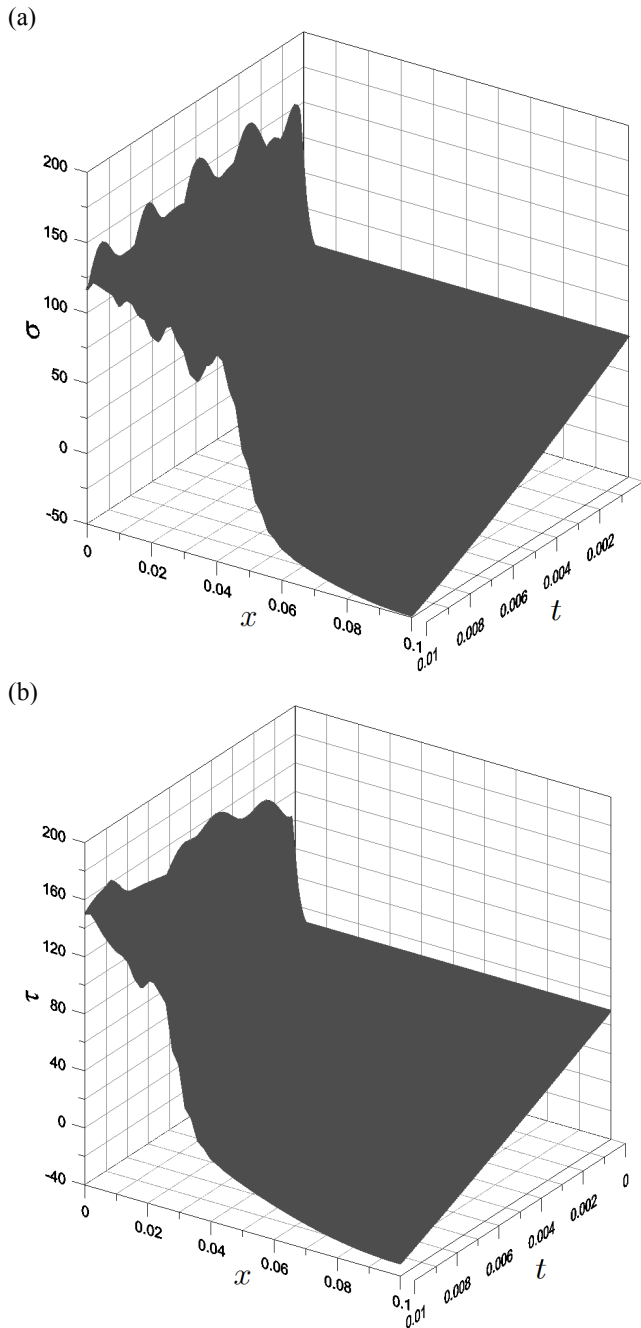


Figure 9: For case 2 of isotropically hardening material the stress wave profiles: (a) axial stress, and (b) shear stress.

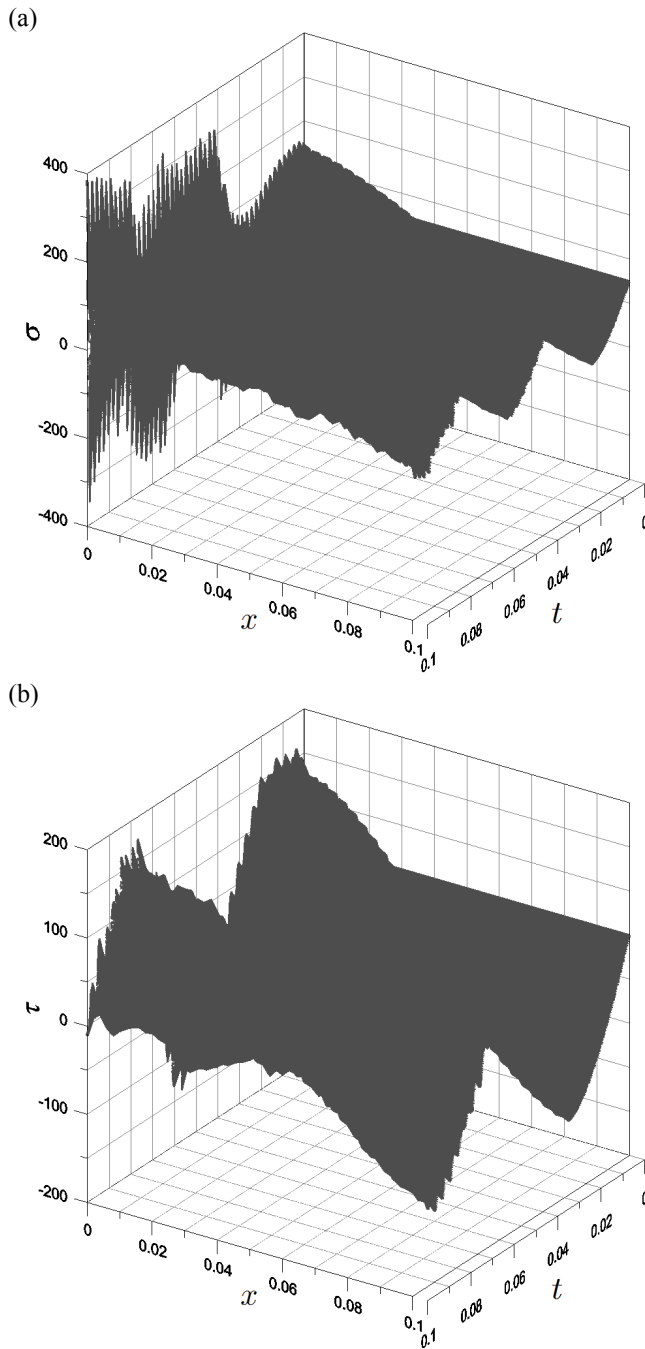


Figure 10: For case 3 of isotropically hardening material the stress wave profiles: (a) axial stress, and (b) shear stress.

unloading state. At point x_2 the material is elastically unloading to compressive stress and negative shear stress.

We solve case 3 under a time stepsize $\delta t = 4 \times 10^{-5}$ sec. In Fig. 2(c) we plot the elastic and plastic zones in the plane (x, t) . In Fig. 7 we plot the waves at some sampled times $t_1 = 10\delta t = 0.0004$ sec, $t_2 = 1500\delta t = 0.06$ sec, $t_3 = 2000\delta t = 0.085$ sec, and $t_4 = 2500\delta t = 0.1$ sec. We plot the time histories of wave at two points $x_1 = 0.002$ and $x_2 = 0.08$ in Fig. 8. It can be seen that at both two points the material behavior is very complex

In Fig. 9 we plot the axial stress and shear stress over the plane (x, t) for case 2, while in Fig. 10 we plot the axial stress and shear stress over the plane (x, t) for case 3. It can be seen that in case 3 the stress distributions are much complicated than that in case 2.

6.3 Linearly hardening material

We let τ_y be a linear function of Λ :

$$\tau_y(\Lambda) = 150 + 100\Lambda. \quad (63)$$

When the right-end of the tube is fixed, the left-end is loaded by impulse stresses. They simultaneously increase parabolically, after that, they keep constant stresses after the interval of rising time $t_r = n_1 \delta t$ where we fix $\delta t = 10^{-5}$ sec:

$$\sigma(0, t) = \begin{cases} \sigma_0 + 2\sigma_f t^2 / t_r^2 & t \in [0, t_r/2), \\ \sigma_0 - 2\sigma_f (t - t_r)^2 / t_r^2 + \sigma_f & t \in [t_r/2, t_r), \\ \sigma_0 + \sigma_f & t \geq t_r, \end{cases} \quad (64)$$

$$\tau(0, t) = \begin{cases} \tau_0 + 2\tau_f t^2 / t_r^2 & t \in [0, t_r/2), \\ \tau_0 - 2\tau_f (t - t_r)^2 / t_r^2 + \tau_f & t \in [t_r/2, t_r), \\ \tau_0 + \tau_f & t \geq t_r. \end{cases} \quad (65)$$

The thin-walled tube is supposed to be pre-stressed to a plastic state with initial conditions $u(x, 0) = 0.3 \cos[(\pi x)/(2\ell)]$, $v(x, 0) = 0.25 \cos[(\pi x)/(2\ell)]$, $\sigma(x, 0) = \sigma_0 = 0$, and $\tau(x, 0) = \tau_0 = 150$ MPa which is equal to the initial shear yield stress 150 MPa. The parameters used are $n_1 = 5$, $\sigma_f = 300$ MPa and $\tau_f = 250$ MPa.

We fix $\Delta x = 0.002$ and solve this problem under a time stepsize $\delta t = 10^{-6}$ sec in a time interval $t \in [0, 0.002]$. In Fig. 11(a) we plot the elastic and plastic zones in the plane (x, t) , where the point corresponding to a plastic state is marked by a black point. In Figs. 11(b) and 11(c) we plot the stress waves at some sampled times $t_1 = 10\delta t = 10^{-5}$ sec, $t_2 = 500\delta t = 0.0005$ sec, $t_3 = 1500\delta t = 0.0015$ sec,

and $t_4 = 2000\delta t = 0.002$ sec. Then we plot the time histories of stress waves at two points $x_1 = 0.002$ and $x_2 = 0.006$ in Figs. 12(a) and 12(b). The stresses path is plotted in Fig. 12(c) and the strains path at the second point is plotted in Fig. 12(d). From Fig. 12(c) it can be seen that at the first point the material quickly tends from point a to point b, which propagates with fast plastic wave, and then from point b to point c along a slow plastic wave. At the second point the material propagate along another fast plastic wave from point a to point d. In Fig. 13 we plot the axial stress and shear stress over the plane (x, t) , from which we can observe the stress distributions.

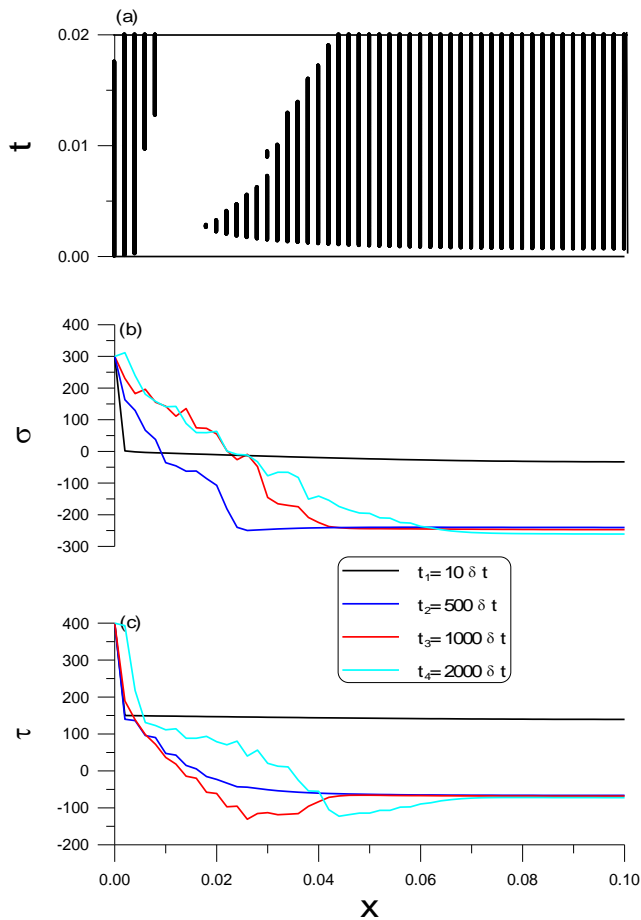


Figure 11: For an isotropically linear hardening material the stress wave propagation: (a) plastic zone, (a) axial stress, and (c) shear stress.

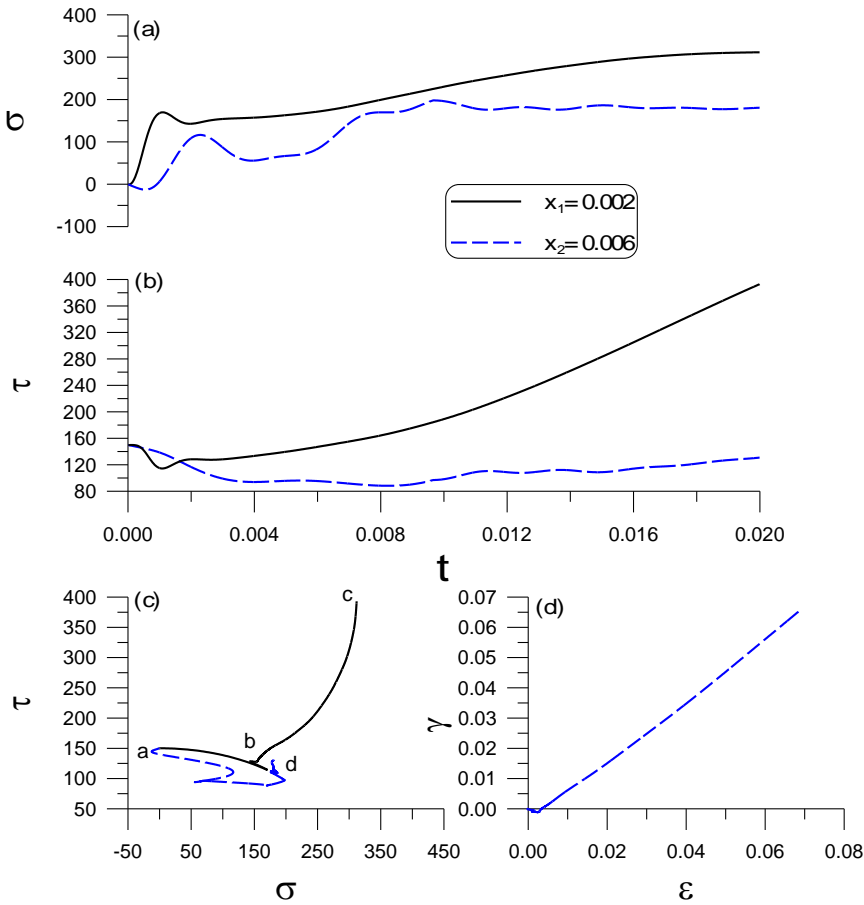


Figure 12: For an isotropically linear hardening material investigating stress wave propagation at two different points: (a) axial stress, (b) shear stress, (c) stress paths, and (d) strain path.

6.4 Isotropically-softening material

Finally we consider an isotropically-softening material with τ_y being a function of Λ :

$$\tau_y(\Lambda) = 50 + 150\exp(-10\Lambda). \tag{66}$$

The initial yield stress is 200 MPa, and then fast tends to 50 MPa.

When the right-end of the tube is fixed, the left-end is loaded by impulse velocities. They simultaneously increase parabolically, after that, they keep constant velocities

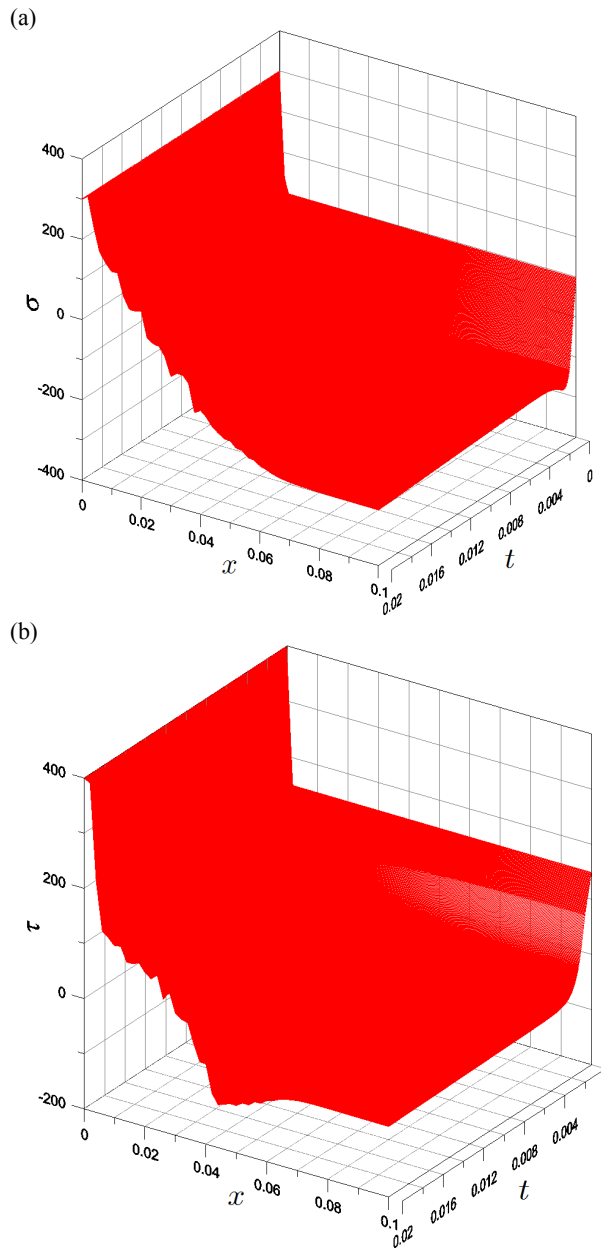


Figure 13: For an isotropically linear hardening material the stress wave profiles: (a) axial stress, and (b) shear stress.

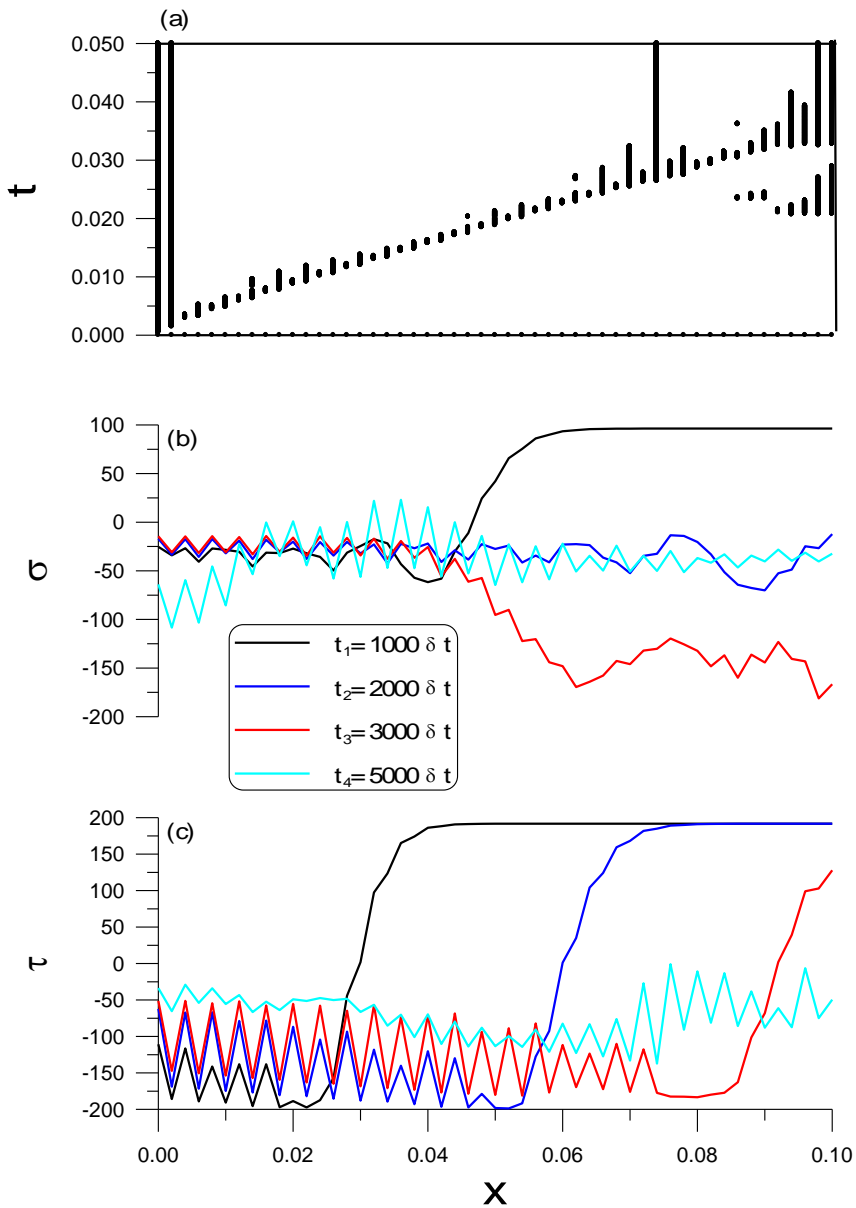


Figure 14: For an isotropically softening material the stress wave propagation: (a) plastic zone, (a) axial stress, and (c) shear stress.

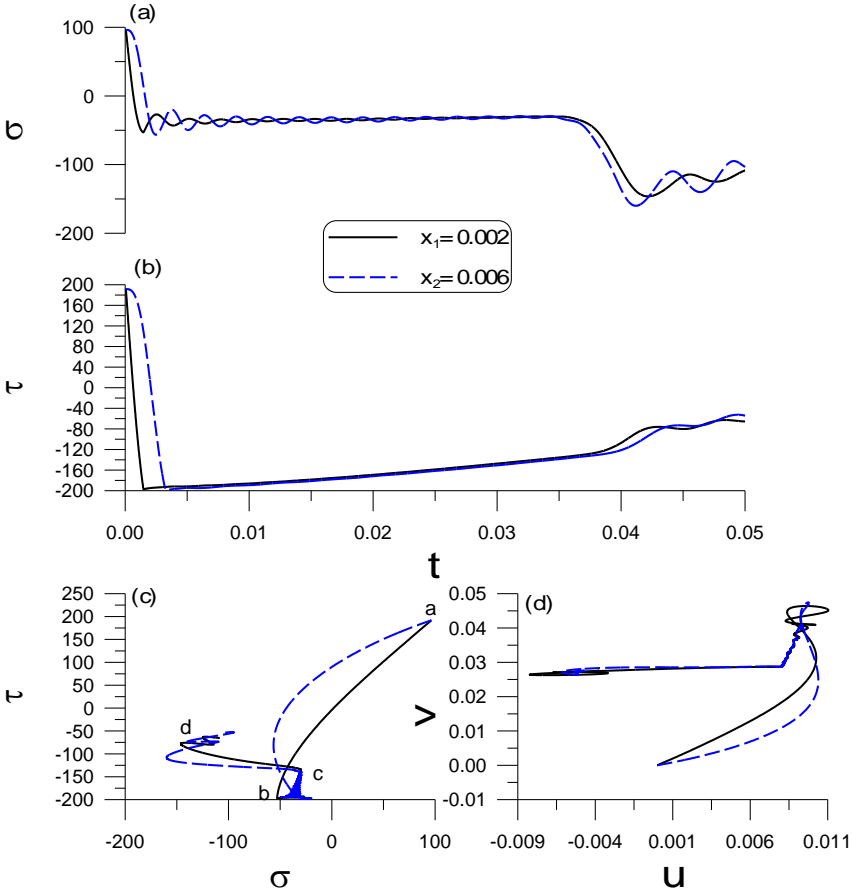


Figure 15: For an isotropically softening material investigating stress wave propagation at two different points: (a) axial stress, (b) shear stress, (c) stress paths, and (d) strain path.

after the interval of rising time $t_r = n_1 \delta t$ where we fix $\delta t = 10^{-5}$ sec:

$$u(0,t) = \begin{cases} 2u_0 t^2 / t_r^2 & t \in [0, t_r/2), \\ -2u_0(t - t_r)^2 / t_r^2 + u_0 & t \in [t_r/2, t_r), \\ u_0 & t \geq t_r, \end{cases} \quad (67)$$

$$v(0,t) = \begin{cases} 2v_0 t^2 / t_r^2 & t \in [0, t_r/2), \\ -2v_0(t - t_r)^2 / t_r^2 + v_0 & t \in [t_r/2, t_r), \\ v_0 & t \geq t_r, \end{cases} \quad (68)$$

where we take $u_0 = 0.01$, $v_0 = 0.05$ and $n_1 = 10$. The thin-walled tube is supposed

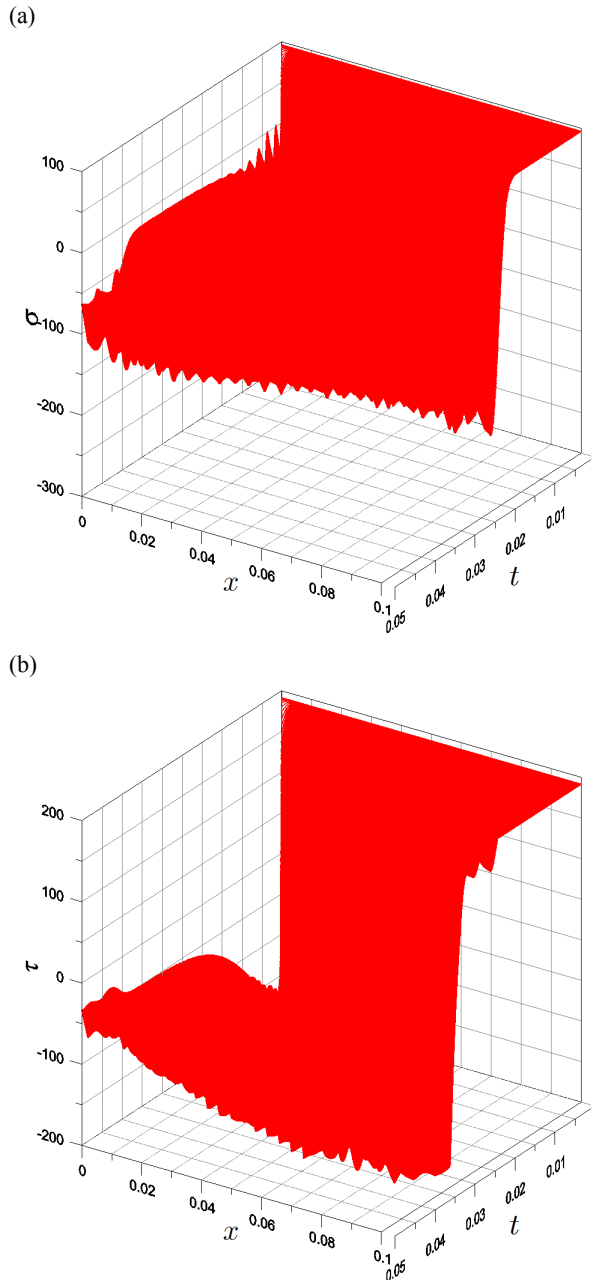


Figure 16: For an isotropically softening material the stress wave profiles: (a) axial stress, and (b) shear stress.

to be pre-stressed to a plastic state with $\sigma(x, 0) = 100$ MPa, and $\tau(x, 0) = 200$ MPa, and other initial conditions are zeros.

We fix $\Delta x = 0.002$ and solve this problem under a time stepsize $\delta t = 10^{-5}$ sec in a time interval $t \in [0, 0.05]$. In Fig. 14(a) we plot the elastic and plastic zones in the plane (x, t) , where the point corresponding to a plastic state is marked by a black point. In Figs. 14(a) and 14 (b) we plot the stress waves at some sampled times $t_1 = 1000\delta t = 0.01$ sec, $t_2 = 2000\delta t = 0.02$ sec, $t_3 = 3000\delta t = 0.03$ sec, and $t_4 = 5000\delta t = 0.05$ sec. Then we plot the time histories of stress waves at two points $x_1 = 0.002$ and $x_2 = 0.006$ in Figs. 15(a) and 15(b). The stresses path is plotted in Fig. 15(c) and the velocity path is plotted in Fig. 15(d). From Fig. 15(c) it can be seen that at the first point the material quickly tends from point a to point b, which propagates with fast plastic wave, and then from point b to point c and then to d along a slow plastic wave. In Fig. 16 we plot the axial stress and shear stress over the plane (x, t) , from which we can observe the stress distributions.

7 Conclusions

The conventional implicit index-two DAEs formulation of plasticity is successfully transformed into a set of explicit index-one DAEs in this paper, for the constitutive equations of an isotropically-hardening/softening material, which provides some advantages such that one can solve the nonlinear elastic-plastic wave propagation problems without resorting on the switching criteria and the two phase equations at each material point. A novel Lie-group differential algebraic equations (LGDAE) method was developed for the solutions of different elastoplastic wave propagation problems, and we found that the LGDAE can faithfully reveal the complex wave behavior of a finite thin-walled tube under different loading conditions and initial conditions, to produce different axial-torsional stress waves. The elastic-plastic wave for the isotropic-hardening-softening material has a complicated feature with many elastic-plastic loadings and unloadings, together with complicated moving elastic-plastic boundaries. Because the LGDAE can provide a very effective time marching solution, without using the two-phase equations and the on-off switch, it can compute the solution straightforward for much saving computational time.

Acknowledgement: Taiwan's National Science Council project NSC-102-2221-E-002-125-MY3 and the 2011 Outstanding Research Award, granted to the first author, are highly appreciated. The work of the second author is supported by a UCI/ARL collaborative research grant.

References

- Büttner, J.; Simeon, B.** (2002): Runge-Kutta methods in elastoplasticity. *Appl. Numer. Math.*, vol. 41, pp. 443-458.
- Büttner, J.; Simeon, B.** (2003a): Büttner J, Simeon B. Differential-algebraic equations in elasto-viscoplasticity. In *Deformation and Failure in Metallic Materials*, Hutter K, Baaser H, Eds., pp. 31-49, Springer, New York.
- Büttner, J.; Simeon, B.** (2003b): Numerical treatment of material equations with yield surfaces. In *Deformation and Failure in Metallic Materials*, Hutter K, Baaser H, Eds., pp. 3-30, Springer, New York.
- Clifton, R. J.** (1966): An analysis of combined longitudinal and torsional plastic waves in a thin-walled tube. In *Proc. 5th U. S. National Congress of Appl. Mech.* ASME, 1966, pp. 465-480.
- Cristescu, N.** (1967): *Dynamical Plasticity*. North-Holland, Amsterdam.
- Eckert, S.; Baaser, H.; Gross, D.; Scherf, O.** (2004): A BDF2 integration method with step size control for elasto-plasticity. *Compu. Mech.*, vol. 34, pp. 377-386.
- Ferris, M. C.; Pang, J. S.** (1997): Engineering and economic applications of complementarity problems. *SIAM Review*, vol. 39, pp. 669-713.
- Giese, G.; Fey, M.** (2003): High-order simulation of the elastic-plastic wave equation in two space dimensions. *Wave Motion*, vol. 38, pp. 327-347.
- Giese, G.; Fey, M.** (2005): A high-resolution residual splitting scheme for the elastic-plastic wave equation. *Wave Motion*, vol. 41, pp. 29-44.
- Goel, R. P.; Malvern, L. E.** (1970): Biaxial plastic simple waves with combined kinematic and isotropic hardening. *ASME J. Appl. Mech.*, vol. 37, pp. 1100-1106.
- Harker, P. T.; Pang, J. S.** (1990): Finite-dimensional variational inequality and nonlinear complementarity problems: A survey of theory, algorithms and applications. *Math. Program*, vol. 48, pp. 161-220.
- Hill, R.** (1950): *The mathematical theory of plasticity*, Oxford University, New York.
- Karagiozova, D.** (2004): Dynamical buckling of elastic-plastic square tubes under axial impact—I: stress wave propagation phenomenon. *Int. J. Impact Eng.*, vol. 30, pp. 143-166.
- Klisinski, M.; Mroz, Z.; Runesson, K.** (1992): Structure of constitutive equations in plasticity for different choices of state and control variables. *Int. J. Plasticity*, vol. 8, pp. 221-243.
- Lin, X.; Ballmann, J.** (1993): A Riemann solver and a second-order Godunov method for elastic-plastic wave propagation in solids. *Int. J. Impact Eng.*, vol. 13,

pp. 463-478.

Lipkin, J.; Clifton, R. J. (1970a): Plastic waves of combined stresses due to longitudinal impact of a pretorqued tube (Part 1: experimental results). *ASME J. Appl. Mech.*, vol. 37, pp. 1107-1112.

Lipkin, J.; Clifton, R. J. (1970b): Plastic waves of combined stresses due to longitudinal impact of a pretorqued tube (Part 2: comparison of theory with experiment). *ASME J. Appl. Mech.*, vol. 37, pp. 1113-1120.

Liu, C.-S. (2005): Computational applications of the Poincaré group on the elasto-plasticity with kinematic hardening. *CMES: Computer Modeling in Engineering & Sciences*, vol. 8, pp. 231-258.

Liu, C.-S. (2006): Computing Prager's kinematic hardening mixed-control equations in a pseudo-Riemann manifold. *CMES: Computer Modeling in Engineering & Sciences*, vol. 12, pp. 161-179.

Liu, C.-S. (2007): Five different formulations of the finite strain perfectly plastic equations. *CMES: Computer Modeling in Engineering & Sciences*, vol. 17, pp. 73-93.

Liu, C.-S. (2013a): A method of Lie-symmetry $GL(n, \mathbb{R})$ for solving non-linear dynamical systems. *Int. J. Non-Linear Mech.*, vol. 52, pp. 85-95.

Liu, C.-S. (2013b): A state feedback controller used to solve an ill-posed linear system by a $GL(n, \mathbb{R})$ iterative algorithm. *Commu. Numer. Anal.*, vol. 2013, Article ID cna-00181, 22 pages.

Liu, C.-S. (2013c): Solving nonlinear differential algebraic equations by an implicit $GL(n, \mathbb{R})$ Lie-group method. *J. Appl. Math.*, vol. 2013, ID 987905, 8 pages.

Liu, C.-S. (2014a): A new sliding control strategy for nonlinear system solved by the Lie-group differential algebraic equation method. *Commun. Nonlinear Sci. Numer. Simulat.*, vol. 19, pp. 2012-2038.

Liu, C.-S. (2014b): Lie-group differential algebraic equations method to recover heat source in a Cauchy problem with analytic continuation data. *Int. J. Heat Mass Transfer*, vol. 78, pp. 538-547.

Liu, C.-S.; Chang, C. W. (2004): Lie group symmetry applied to the computation of convex plasticity constitutive equation. *CMES: Computer Modeling in Engineering & Sciences*, vol. 6, pp. 277-294.

Nadai, A. (1950): *Theory of Flow and Fracture of Solids*. McGraw-Hill, New York.

Nowacki, W. K. (1978): *Stress Waves in Non-elastic Solids*. Pergamon Press, New York.

Tanimoto, N. (2007): An analysis of combined longitudinal and torsional elastic-plastic-viscoplastic waves in a thin-walled tube. *J. Solid Mech Mater. Eng.*, vol. 1, pp. 1112-1127.

Ting, T. C. T. (1969): Interaction of shock waves due to combined two shear loadings. *Int. J. Solids Struct.*, vol. 5, pp. 415-435.

Ting, T. C. T. (1972): The initiation of combined stress waves in a thin-walled tube due to impact loadings. *Int. J. Solids Struct.*, vol. 8, pp. 269-293.

Ting, T. C. T. (1973): Plastic wave speeds in isotropically work-hardening materials. *ASME J. Appl. Mech.*, vol. 40, pp. 1045-1049.

Wu, H. C.; Lin, H. C. (1974): Combined plastic waves in a thin-walled tube. *Int. J. Solids Struct.*, vol. 10, pp. 903-917.

Yang, C. Y. (1970): Strain hardening effect on unloading spherical waves in an elastic plastic medium. *Int. J. Solids Struct.*, vol. 6, pp. 757-772.